Review

Computational inhibitor design against malaria plasmepsins

S. Bjelic[a,†], M. Nervall[a,†], H. Gutiérrez-de-Terán[a], K. Ersmark[b], A. Hallberg[b] and J. Åqvist[a,*]

[a] Department of Cell and Molecular Biology, Uppsala University, Biomedical Center, Box 596, SE-751 24
Uppsala (Sweden), Fax: +46 18 53 69 71, e-mail: aqvist@xray.bmc.uu.se
[b] Department of Medicinal Chemistry, Uppsala University, Biomedical Center, Box 574, SE-751 23 Uppsala
(Sweden)

Abstract. Plasmepsins are aspartic proteases involved in the degradation of the host cell hemoglobin that is used as a food source by the malaria parasite. Plasmepsins are highly promising as drug targets, especially when combined with the inhibition of falcipains that are also involved in hemoglobin catabolism. In this review, we discuss the mechanism of plasmepsins I–IV in view of the interest in transition state mimetics as potential compounds for lead development. Inhibitor development against plasmepsin II as well as relevant crystal structures are summarized in order to give an overview of the field. Application of computational techniques, especially binding affinity prediction by the linear interaction energy method, in the development of malarial plasmepsin inhibitors has been highly successful and is discussed in detail. Homology modeling and molecular docking have been useful in the current inhibitor design project, and the combination of such methods with binding free energy calculations is analyzed.

Keywords. Malaria, plasmepsin, inhibitor design, reaction mechanism, molecular dynamics, linear interaction energy method.

Introduction

Malaria is still one of the most widespread and lethal diseases in the world, affecting the tropical parts of the globe, with Africa being the most plagued continent. Every year there are more than 500 million clinical cases of malaria and several millions of them are children [1]. Emerging drug resistance and the lack of a functioning vaccine are two main reasons behind the failure to control and eradicate the disease [2–6]. The malaria parasite life cycle is highly complex and is characterized by many different life stages in the human and the mosquito host. For example, one of the major reasons for the large number of clinical cases in Africa is caused by longevity of the mosquito vector, *Anopheles gambiae* [4]. Infection in the human host starts with a mosquito injecting sporozoites that travel by the blood stream to the liver where they invade the liver cells. This leads to the development and release of merozoites that infect red blood cells where they proliferate. The rupture of the red blood cells and the release of new merozoites into the blood stream is the direct cause of the typical malaria fever. Four species of *Plasmodium* are known to infect humans: *falciparum*, *malariae*, *ovale* and *vivax*. *P. falciparum* is by far the most deadly of the human malaria species and has the highest priority in the search for effective drugs. *P. vivax* is less efficient than *P. falciparum* in the invasion

---

† These authors contributed equally to this work.
* Corresponding author.

of red blood cells, and with this slight difference in parasite biology, *vivax* malaria is less lethal [7].

The global effort to defeat malaria has expanded greatly in the last few years. In this process, a number of novel strategies to obstruct malarial growth have emerged. Among the most appealing strategies is an attempt to produce a long-lasting vaccine which would help eradicate the disease [8]. The vaccine developed by Alonso et al. [9] appears promising, but has so far only given limited protection [9]. Until there is a vaccine on the market offering full protection against malaria, we must consider therapeutic drugs for preventive chemotherapy and treatment of acute malaria. However, a problem with present drugs is growing resistance. The limited number of malaria drugs and their extensive use has led to increasing resistance among malaria strains. Hence, drugs with novel mechanisms of action are desperately needed to combat the disease. In the wake of the full genome sequencing of *P. falciparum*, numerous new drug targets have been proposed. These are quite diverse and include enzymes from the respiratory chain in the parasite mitochondria [10, 11], several transport proteins [12, 13], enzymes in the fatty acid synthetic pathway [14], a number of proteases [15–17] and DNA replication and regulation [18].

A trend among ongoing projects is to recycle drugs and knowledge from previous lead developments. For example, Yanow et al. [18] have studied alkylation of DNA by adozelesin. The compound was originally an anti-tumor drug that targets A/T-rich regions in the DNA. Remarkably, the drug prevents malaria parasite growth in a mouse model of malaria without killing the mice. Further examples of lead recycling can be found among protease inhibitors, where lead compounds can be extracted from a large group of FDA-approved drugs for AIDS. The proteases from the malaria parasite, named plasmepsins (Plm), have previously been validated as potential drug targets [19–21]. However, recent results from knock-out experiments raise questions regarding the validity of plasmepsins as single drug targets [22]. Liu et al. [22] have validated plasmepsins together with falcipains, another protease family that is involved in hemoglobin degradation, during the intraerythrocytic life stage when the parasite is dependent on the hemoglobin as the external food source. The authors concluded that the doubling time for the malaria parasite was longer for the plasmepsin/falcipain knock-out (plasmepsin I, plasmepsin IV and falcipain-2) than for either plasmepsin or falcipain knock-outs alone. Furthermore, the aspartic protease inhibitor pepstatin A was highly potent against falcipain knock-out. Thus plasmepsin inhibitors could potentially be part of an effective drug cocktail in combination with falcipain inhibitors [22]. Several scaffolds from AIDS drug discovery projects have been reused to aid malaria drug development [23, 24]. In this article, we will review the advances of computational approaches in inhibitor development, with a special focus on plasmepsin inhibitor design.

Computational approaches in inhibitor development

Computational chemistry has gained considerable influence on the drug design process during the last decades [25, 26]. Development of faster computers and improvement of theoretical methods have together contributed to the rapid progression of the field. The theoretical methods used in computer-aided drug design range from statistical approaches such as quantitative structure–activity relationships (QSARs) to structure-based techniques including molecular docking and free energy calculations. Here, we will focus on the latter, and illustrate their usefulness in the ligand design process.

Approaches used in structure-based ligand design usually include some docking algorithm to predict conformations of inhibitor complexes, followed by a method to estimate the binding affinity. Popular programs for docking include AutoDock [27], Dock [28], FlexX [29], Glide [30, 31] and Gold [32, 33]. The programs differ slightly in methodology but generally have an algorithm that at least allows full flexibility of the ligand while the receptor is kept rigid. The search space would usually become unreasonably large if full receptor flexibility were included. The search algorithm is coupled to a scoring function that ranks the conformations from the search. In addition, the ligands can be ranked relative to each other by the same scoring function, or some other method that can estimate free energies of binding from structural information.

Techniques to determine binding affinities span from rigorous statistical mechanical methods that rely on conformational sampling by molecular dynamics or Monte Carlo to methods optimized for speed, such as empirical or knowledge-based scoring functions. Empirical and knowledge-based scoring functions are parameterized on large datasets of three-dimensional (3D) ligand-protein structures to reproduce binding free energies. The knowledge-based functions, rather than employing a designed equation, make use of statistical structural information available in the Protein Data Bank (PDB) to derive pairwise atom-atom interaction terms. Although scoring functions are easy to use and can screen large libraries of compounds, they have difficulties in ranking ligands with small differences in chemical structure, *e.g.* in

lead optimization. The resulting binding affinities from scoring functions are often associated with errors of the order of 2.5 kcal/mol [34]. Hence, the prime use of scoring functions as a tool for ranking ligands is limited to relative rankings of ligands covering a broad spectrum of affinities, for example in lead identification. Some scoring functions that are widely used are Chemscore [35], Xscore [36], Drugscore [37] and Goldscore [32].

More thorough methods are required when the differences between the ligands in a series are more subtle, *e.g.* in the case of small substitutions on a conserved scaffold. These methods are generally based on thermodynamic and physical principles. Two examples are free energy perturbation (FEP) and thermodynamic integration (TI), both of which calculate the difference in free energy of binding between two ligands by transforming one ligand to the other. However, the use of FEP/TI is limited to calculations of relative binding energies between pairs of molecules with only minor structural differences [38]. The transformation between the ligands requires extensive sampling and these methods are therefore quite time consuming. Furthermore, FEP/TI is not likely to be successful when perturbations can end up in different local conformational minima separated by high barriers, because interconversion between binding and nonbinding conformations is unlikely to occur during limited simulation time [39]. Due to these problems, FEP/TI is often of limited use in the drug design process.

In the intermediate regime between FEP/TI and scoring functions, both in terms of level of theory and time requirements, there are a number of additional techniques. One is the linear interaction energy (LIE) method developed by Åqvist and co-workers [40] (see the Theoretical methods section for technical details). LIE has been successfully applied in several projects addressing ligand binding as well as protein-protein interactions [38, 41, 42], and has inspired other related methods [43–46]. Two examples are SGB-LIE [45] and LIECE [43], both of which treat the solvent as a continuum, compared to LIE where water molecules are explicitly represented. The linear response approximation (LRA)-based method proposed by Warshel and co-workers is also a simplification of the FEP method with a subtle difference in the treatment of the electrostatic contribution [47, 48]. Another approach for affinity estimations in the same regime of complexity is the MM-PBSA method, which combines molecular mechanics (MM) energies with Poisson Boltzmann (PB) treatment of the electrostatics and surface area (SA) calculations to account for the nonpolar interactions [49]. All these methods are useful in the process of lead optimization as they are generally accurate enough to discriminate between good and bad binders of chemically related compounds. However, they are not fast enough to scan entire libraries, rendering them unsuitable for virtual screening purposes. An additional benefit of the methods is that the sampling of the ligand–receptor complex allows for a straightforward rationalization of the calculated free energies of binding. Moreover, the electrostatic and nonpolar components of binding are calculated, and their separate contributions can be assessed. In case of the LIE method, for example, a recent thermodynamic analysis of the components of binding has been reported that examines the treatment of entropy effects [50].

A number of successful examples exist where computational chemistry has made significant contributions to the processes of lead discovery and optimization. Evaluation of binding free energies for diverse sets of inhibitors, and the separation of the energy components, was invaluable to the organic chemists in the current project for rational design of plasmepsin inhibitors [16, 23, 51–55]. Haque et al. [56] used a combination of fragment docking techniques and synthetic combinatorial library design to find low-nanomolar inhibitors of Plm. Inhibitors of dihydrofolate reductase are used in the treatment of a number of diseases, both as antifolates for the human enzyme and for alleviating opportunistic infections. Theoretical methods, for example applied docking/scoring (utilizing AutoDock) and FEP/LIE, have been applied successfully in the development of potential drug concepts and to gain insights into inhibitor binding to dihydrofolate reductase [57–60]. Reverse transcriptase, an HIV drug target, has been studied in detail by computational chemistry techniques (such as LIE), with progress towards design of efficient inhibitors [61–64]. A study has recently been reported for the human β-secretase BACE-1, the membrane-bound aspartic protease implicated in Alzheimer's disease. In this case, high-throughput docking was followed by estimations of ligand binding free energies using LIECE [65]. A further example of successful use of binding free energy predictions in the rationalization of binding requirements has been reported for a series of human cathepsin D inhibitors [66] using the MM-PBSA method [67, 68]. Moreover, by an entirely computational approach, Becker *et al.* [69] used 3D modeling of a GPCR and high-throughput screening (HTS) to find novel lead compounds. During the lead optimization process, each compound was thoroughly assessed through computational methods and only 31 compounds were synthesized. The authors managed to find an approach that produced a compound that made phase III clinical trials within 30 months from the project start.

Computational methods have the advantage of being faster and far less expensive than standard HTS. However, the complex nature of medicinal chemistry is difficult to predict. This is the case especially when predicting biological effects *in vivo*, where many aspects come into play, *e.g.* bioavailability and metabolism. Nevertheless, computational methods provide a powerful complement to standard HTS and by combining chemical screening with computational tools, lead discovery and optimization can be made significantly more cost and time effective. In this review, we will discuss our recent efforts to develop potent plasmepsin inhibitors, with a focus on lead optimization. In projects like malaria treatment where budgets may be very limited, computational methods provide a very cost-effective approach for ligand design. A number of common problems in medicinal chemistry have been addressed in the present project: (i) the identification of a transition state mimetic [70, 71], (ii) the selection of active stereoisomers in the process of lead scaffold identification [23], (iii) optimization of inhibitor side chains for improved binding [51], (iv) bioisostere replacement and macrocyclic protection of amide bonds, to improve pharmacokinetic properties [16, 52] and (v) exploration of multiple enzyme inhibition and selectivity issues [54].

Reaction mechanism and inhibitor development

The genome sequencing of *P. falciparum* has lead to the identification of ten different genes encoding plasmepsins [72], numbered Plm I to Plm X. Plm I–IV are situated in the acidic food vacuole and are active during the intraerythrocytic phase of the life cycle, providing nutrients for parasite growth. In particular, these enzymes are involved in the degradation of host hemoglobin, and as such constitute possible drug targets. Plm V, IX and X are expressed concurrently with Plm I–IV, but are not transported to the food vacuole. The remaining plasmepsins (Plm VI, VII, VIII) are not expressed during the intraerythrocytic stage [73]. The plasmepsins are aspartic proteases with a pepsin like fold (Fig. 1a) [74]. These enzymes are composed of two domains with the active site situated in a deep cleft in between and a loop (the flap) that covers the active site. In contrast, retroviral proteases, for example HIV-1 protease, consist of two identical subunits with two equivalent flaps covering the active site (Fig. 1b) [75]. Upon substrate binding to this class of enzymes, the flap (or flaps in HIV-1 protease) closes around a substrate part containing the scissile bond, thereby forming a solvent-shielded environment inside the enzyme. Between the flap region and the substrate, a structurally conserved

water molecule is situated in HIV-1 protease [75] which is lacking in Plm II. The apparent lack of symmetry in Plm II can be deceiving, as very potent symmetrical inhibitors against it have been designed [51]. Each domain in plasmepsins contributes an aspartic acid residue to the active site, except for the histo-aspartic protease (HAP, corresponding to Plm III), in which one of the catalytic aspartates is mutated to a histidine residue [70, 73, 76]. The peptide bond of the substrate is cleaved in Plm I–IV by a catalytic aspartate (Fig. 2) that acts as a general base by activating a water molecule through abstraction of a proton. The resulting hydroxide ion attacks the peptide bond forming a transient tetrahedral intermediate. It has also been shown that the formation of a tetrahedral intermediate can occur via a concerted path during which the hydroxide ion is not completely formed [70, 71]. Breakdown of the transient tetrahedral intermediate species is preceded by proton transfer to the amide nitrogen from the aspartate previously involved in water protolysis. The originally neutral aspartic residue (or charged histidine in HAP) stabilizes the negative charge developing on the amide carbonyl oxygen. It is also possible that during this stabilization, the proton may be transiently transferred to the tetrahedral oxyanion, forming a short-lived diol intermediate.

Inhibitors are generally designed to resemble the structure of a molecular species occurring during the reaction. A powerful way to characterize high-energy intermediates is to simulate the reaction mechanism by quantum mechanics/molecular mechanics (QM/MM) methods. Bjelic and Åqvist [70, 71] have, for example, determined the reaction energetics and intermediates for *P. falciparum* Plm II and HAP (Fig. 2 and Fig. 3) [70, 71]. Reaction free energy profiles were generated through molecular dynamics FEP simulations in combination with the empirical valence bond (EVB) method. The EVB approach is well documented and has been used successfully for more than two decades in theoretical investigations of enzyme catalysis [77, 78]. Compared to *ab initio* and semi-empirical molecular orbital QM/MM methods [79], the greatest advantage of EVB is that it lends itself to accurate calibration by parameterization against a suitable uncatalyzed reference reaction in water to reproduce experimental or high-level *ab initio* energetics.

The formation and breakdown of the transient tetrahedral intermediate was simulated both in a stepwise and concerted manner for HAP, while in Plm II, only the concerted tetrahedral intermediate formation was considered. Breakdown of the tetrahedral intermediate in Plm II was further modeled as stepwise, with the proton fully transferred to the
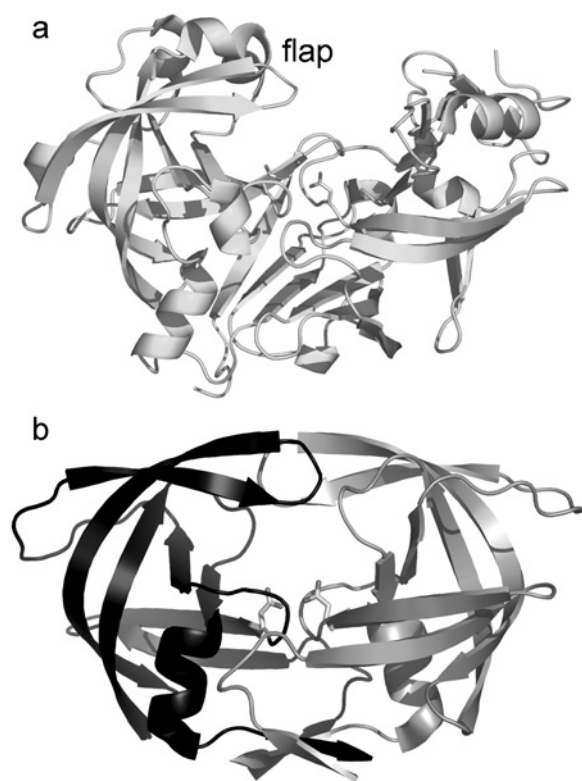
Figure 1. Aspartic proteases plasmepsin II [86] (*a*) and HIV-1 protease [97] (*b*) cleave peptides by the use of two aspartic acid residues situated in the active site. Plasmepsin II consists of two domains while HIV-1 protease is a dimer as indicated by the different shading of the subunits.

peptide nitrogen before dissociation. In Figure 2, the free energy profiles for the concerted formation of the tetrahedral intermediate and its stepwise breakdown are presented for Plm II and HAP as well as for the uncatalyzed water reaction. The experimental reac-

tion rates for both Plm II and HAP were well reproduced and the catalytic effect of the enzymes, with more than 10 kcal/mol stabilization of the high-energy regime, is clearly evident. These results not only give insights into the reaction energetics, but also provide structural information along the reaction path, which is valuable for inhibitor development. The high resemblance bewteen the tetrahedral intermediate structure and one of the inhibitors reported by Ersmark et al. [52] can be seen in Figure 3a,b. The interactions present between the tetrahedral intermediate and Plm II are important for inhibitor design, especially the substrate/inhibitor hydrogen bonds that confer specificity, while side chains can generally be varied to improve the overall binding affinity (Fig. 3c). The oxyanion of the tetrahedral intermediate transiently formed during peptide hydrolysis in HAP (Fig. 3d) [70] is stabilized by a positively charged histidine (His34). This histidine has replaced the corresponding protonated aspartic acid (Asp34) in Plm II that stabilizes the tetrahedral intermediate in a similar manner. This is the first enzyme with this type of active site that has been characterized. Since the structure was not available, state-of-the-art computational methods were employed to establish the reaction mechanism. A homology model of HAP was constructed using the SWISS-MODEL [80] modeling server and it was subsequently refined by molecular dynamics simulations. The substrate conformations were also unknown and were determined by automated docking procedures as implemented in AutoDock3 [27]. Two possible substrate conformations, giving rise to catalysis with rates compatible to experiments, were found. The first conformation of the peptide substrate was an extended linear form and the second conformation was similar to that of the
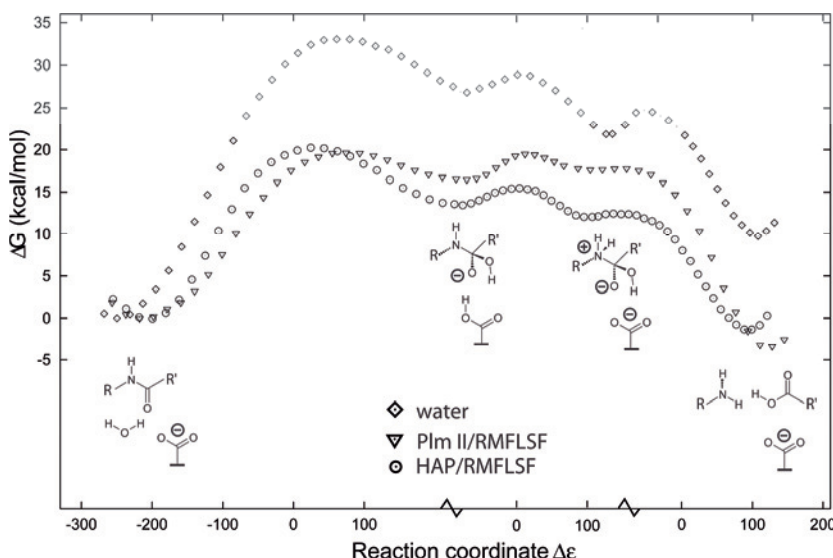

Figure 2. Free energy profiles for peptide hydrolysis in plasmepsins, Plm II and HAP, and in water were determined by molecular dynamics (MD) free energy perturbation (FEP) simulations in combination with the empirical valence bond (EVB) method. The schematic reaction pathway involving different transient intermediates is shown along the free energy profiles. The initially unprotonated catalytic aspartate acts as a general acid/base for peptide cleavage, and stabilization of the oxyanion is mainly achieved by the neutral aspartic acid and charged histidine in Plm II and HAP, respectively. RMFLSF is a peptide substrate in the enzymes, while the water reaction refers to dipeptide hydrolysis (FL and AA).
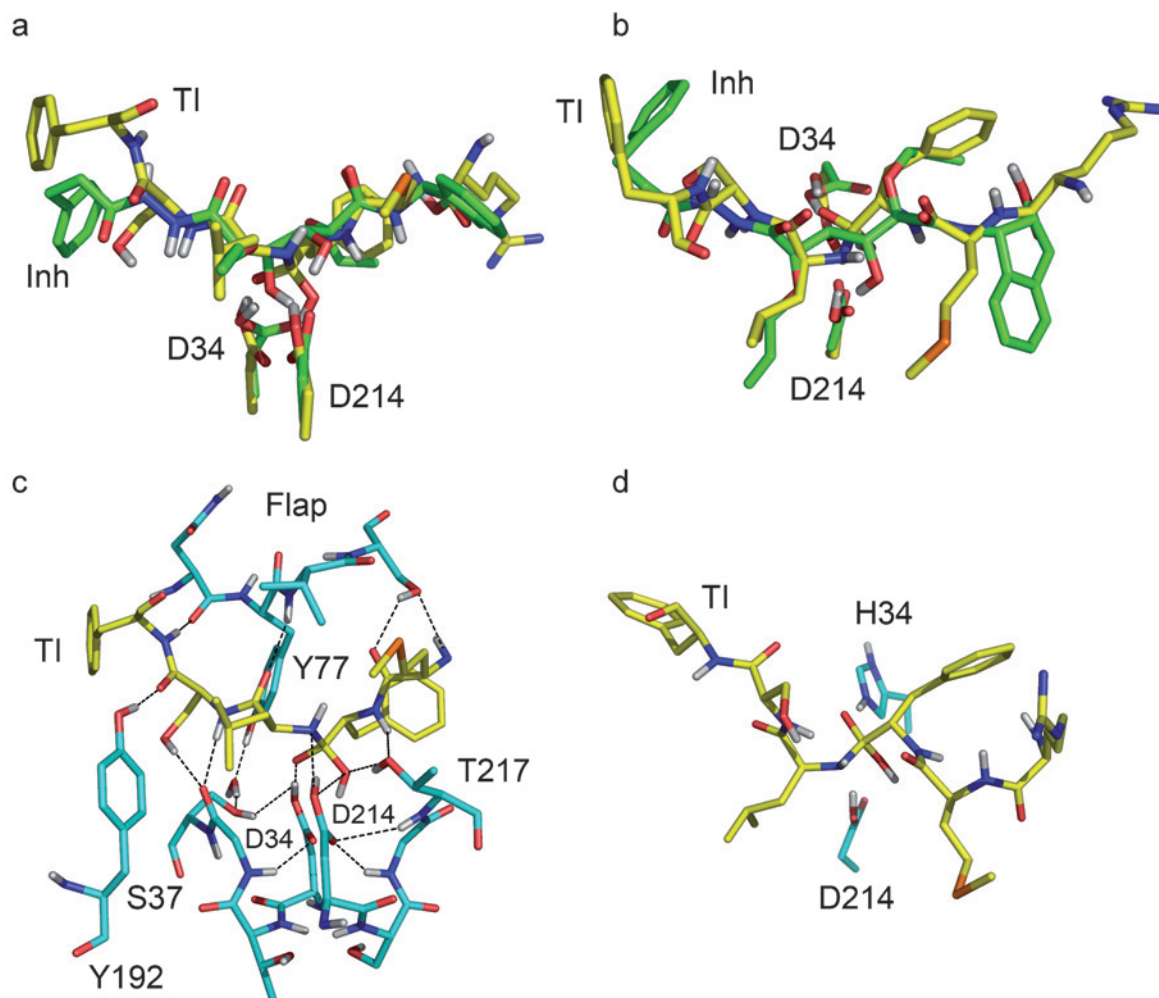
Figure 3. Inhibitor **15** in Table 1 mimics the tetrahedral intermediate (TI) remarkably well (*a, b*). In *a*, the side view is presented with catalytic aspartates interacting with the inhibitor hydroxyl groups or tetrahedral intermediate hydroxyl and oxyanion. In the top view (*b*), the inhibitor side chains occupy approximately the same space as in the tetrahedral intermediate. The catalytic aspartates, D34 and D214, are responsible for peptide hydrolysis in Plm II (*c*), while D34 is mutated to a histidine in HAP (*d*). The structures are obtained from MD simulations [52, 70, 71].

corresponding six-amino-acid fragment in the native hemoglobin structure [see Fig. 1 in 70]. The extended conformation was finally predicted to be the active one, due to its lower internal energy. Although homology models are obviously associated with uncertainties regarding fine details of the structure, if such models are refined and sampled by MD simulations and the information is incorporated in the final model, they can be very useful for understanding structure–activity relationships as in the HAP enzyme case [70].

The tetrahedral intermediate in Plm II can serve as a useful structure for rationalizing the potency of several reported Plm II inhibitors. The fact that these are designed to mimic the transition state, or the closely related tetrahedral intermediate, is evident from Figure 4 (structures a, b, d and f) [53, 81]. The

inhibitors b, d and f in Figure 4 all have a central hydroxyl group that interacts with the catalytic aspartates. The scaffold in structure a even has two hydroxyl groups, in the 1,2-dihydroxyethylene moiety, that make strong hydrogen bonds with the catalytic aspartates. The aminopiperidine compound in structure c, in contrast, is a novel type of plasmepsin inhibitor that targets plasmepsins with the flap loop in the open conformation, i.e. before it folds and closes around the substrate (*cf.* Fig. 3c). Moreover, the amide in this scaffold does not interact with the catalytic aspartates but, instead there is a water molecule bridging the interactions to the nitrogen in the six-membered ring [82]. The remaining two scaffolds, diamine-clamp and arylpiperidine-based inhibitors (Fig. 4, structures e and g), stand out as they clearly do not resemble either the transition state or the
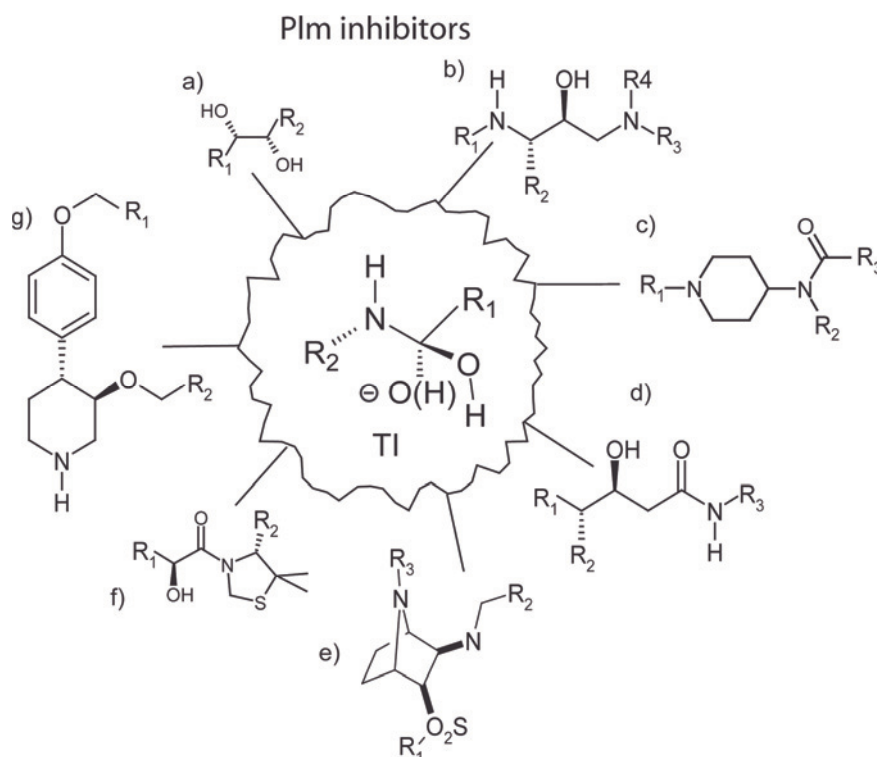
Plm inhibitors

scissile substrate amide. Arylpiperidines originate from renin inhibitors, and are an additional example where the aspartic protease scaffolds from other research areas are reused for novel purposes [81]. The diamine-clamp inhibitors (Fig. 4, structure e) interact with the flap in the open conformation as proposed by Hof et al. [83]. In that respect they are more similar to aminopiperidine inhibitors (Fig. 4, structure c), compared to compounds based on scaffolds in Figure 4, structures a, b, d, f and g. The tetrahedral intermediate/substrate-mimetic inhibitors generally extend on both sides of the catalytic center, and are intended to optimally fill the S1-S3 and S1′-S3′ subsites (Fig. 5). This extension of the ligand is not only important for affinity, but also to a high degree determines the selectivity through the hydrogen-bonding pattern and shape complementarity with the rest of the active site upstream and downstream from the catalytic core [54, 84].

Among the plasmepsins, Plm II has been the most extensively characterized, with a number of X-ray structures reported [82, 85–88]. These were co-crystallized with several different hydroxyethylamine/statin-based inhibitors as well as an achiral inhibitor [82, 85, 86] (Fig. 6). The structures of uncomplexed plasmepsin [86] and proplasmepsin have also been determined [87]. Several structures pending publication have further been deposited in the PDB (1M43, 1ME6, 1XDH, 1XE5, 1XE6, 1W6H
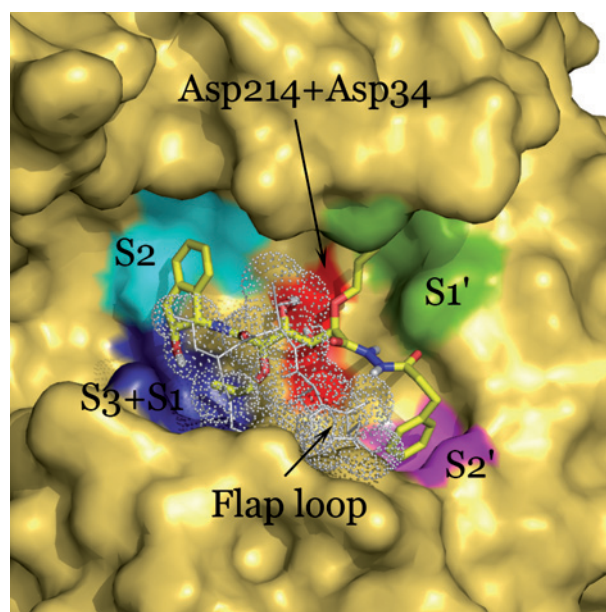

Figure 5. Representative MD snapshot of inhibitor **15** in Table 1 bound to Plm II [52]. Residues 76–80, the flap loop region, are represented by lines and dots. The subsites of the receptor are colored, with S1 and S3 in blue, S2 in cyan, S1′ in green and S2′ in magenta. The red patch shows the location of Asp34 and Asp214.

and 1W6I). Most of them are complexed with pepstatin A or statin-based inhibitors. More recently, Plm IV has also captured the attention as a drug target, when it was found that deletion of Plm I and

Plm IV genes reduced malaria parasite growth rate [20]. Further, recent reports show that poly-inhibition of plasmepsins, and other proteases such as falcipains, may be desirable in potential antimalarials to ensure clinical efficacy [21, 22].
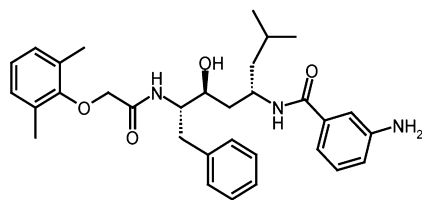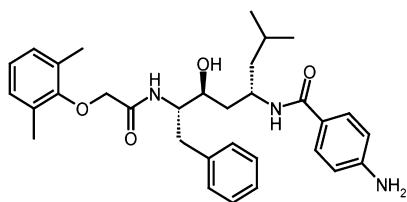
pepstatin A
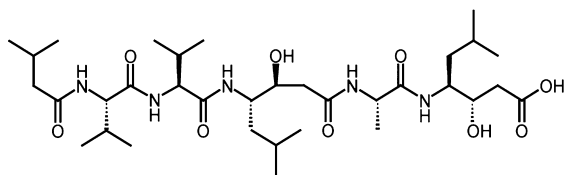
EH58
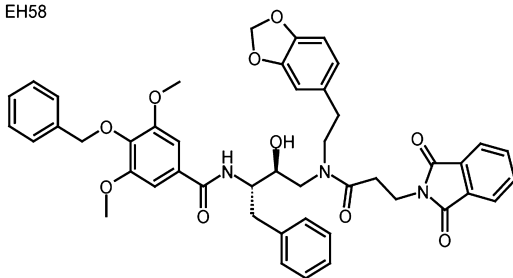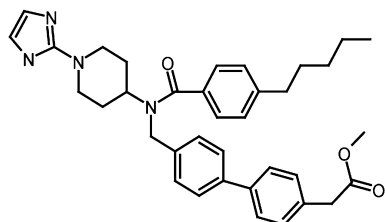
rs367

rs370

achiral inhibitor

Figure 6. Plasmepsin II structures complexed with statin/hydroxyethylamine-based inhibitors (pepstatin A, EH58, rs367 and rs370) [85, 86, 88] and an achiral inhibitor [82] that have been determined by X-ray crystallography.

Using the MD/LIE method in the design of Plm II inhibitors

The starting scaffold for development of potential plasmepsin inhibitors in this project was the symmetrical 1,2-dihydroxyethylene transition state mimetic (see Fig. 3 and Fig. 4, structure a) [23]. Bislactones were initially allylated or bensylated, and subsequently the rings were opened using either D- or L-valine. Chemical synthesis of the scaffold resulted in different stereochemical configurations with six stereocenters, denoted with stars in compounds **1** and **2** in Table 1. Different stereoisomers are generally expected to have quite different binding profiles and considerable research resources can be saved by predicting the most active stereoisomer by computational means. Hence, the stereoisomer characteristics were evaluated by MD simulations, and LIE was employed to determine the binding affinities. Starting structures for the MD simulations were constructed by manually superimposing the transition state mimic scaffold onto the inhibitor backbone of a structure of Plm II in complex with pepstatin A (1SME). The same stereochemistry (*SRRRRS*) was predicted to be the most active one in both the benzyloxy and the allyloxy compound series and, furthermore, the predicted stereochemistry is compatible with the substrate stereochemistry. Thus, the best stereoisomer is, not surprisingly, a mimic of a peptide chain with natural amino acids. Moreover, the calculated affinities for the best stereoisomers were in good agreement with experimental values (**1** and **2** in Table 1).

In the analysis of the MD simulations, several key interactions were found between the inhibitors and Plm II. The two central hydroxyl groups of the ligands were found to hydrogen bond to the aspartic acid that was considered negatively charged (Asp214). Furthermore, the hydroxyl on the prime side was found to accept a hydrogen bond from the protonated aspartic acid. Another conserved key interaction was discovered between the hydroxyl on the nonprime side and a water molecule. The water molecule was found to be hydrogen bonded to the hydroxyl of Thr217, thereby bridging from the enzyme to the ligand.

When the optimal stereochemistry of the inhibitor scaffold had been established, the next step was to improve overall binding by optimizing the interactions in the P2/P2′ position of the ligands [23]. This was done by introducing a (1*S*,2*R*)-1-amino-2-indanol instead of valine methylamide in the allyloxy compound **1**. The resulting compound, **3** in Table 1, presented a 50-fold increase in binding affinity. The main contribution to the higher affinity of **3,** as compared to **1**, was due to an increase in the nonpolar component of the free energy of binding. The electro-

Table 1. Calculated and experimental binding free energies for Plm II and Plm IV inhibitors.

Compound	Structure	ΔG_{bind} (kcal/mol)			
		Plm II		Plm IV	
		experimental[1]	LIE[2]	experimental[1]	LIE[3]
1[4]		−7.4	−6.8± 0.4	–	–
2[4]		−7.4	−8.6± 0.4	–	–
3		−9.6	−9.1± 0.4	–	–
4		−9.7	−9.6± 0.3	–	–
5		> −7.7	> −2.2[5]	–	–
6		−10.3	−8.5± 0.5	–	–

Table 1 *(Continued)*

Compound	Structure	ΔG_{bind} (kcal/mol)			
		Plm II		Plm IV	
		experimental[1]	LIE[2]	experimental[1]	LIE[3]
7		−11.3	−12.2 ± 0.4	–	–
8		−10.8	−10.1± 1.13	–	–
9		−9.3	−10.8± 0.5	–	–
10		−9.4	−10.1 ± 1.0	–	–
11		−8.9	−8.4 ± 0.8	–	–

Table 1 *(Continued)*
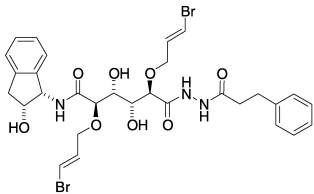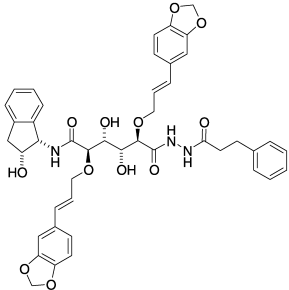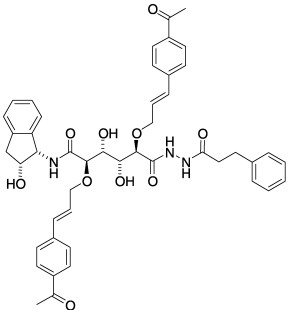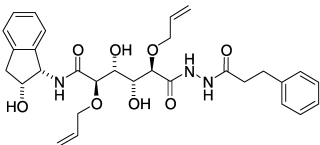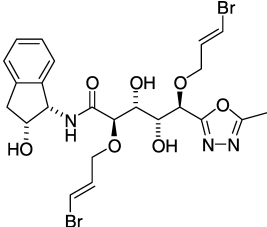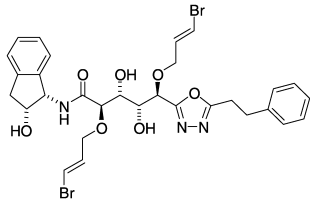
Compound	Structure	ΔG_{bind} (kcal/mol)			
		Plm II		Plm IV	
		experimental[1]	LIE[2]	experimental[1]	LIE[3]
12		−11.2	−10.2 ± 1.1	−7.8	−8.4 ± 0.4
13		−10.9	−10.6 ± 1.3	−8.8	−8.3 ± 0.3
14		−9.4	−10.9 ± 1.0	–	–
15		−9.3	−9.7 ± 0.7	–	–
16		−7.3	−6.9 ± 0.5	−6.9	−6.3 ± 0.5
17		−7.6	−8.4 ± 0.2	−6.8	−7.0 ± 0.3

Table 1 *(Continued)*
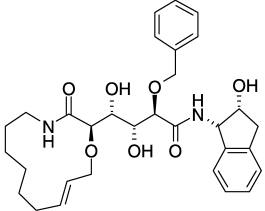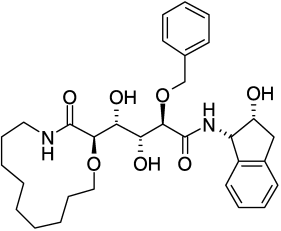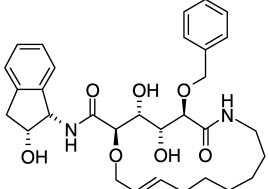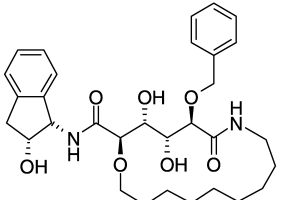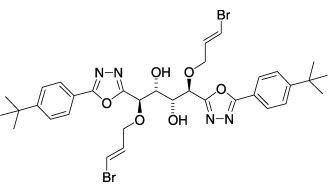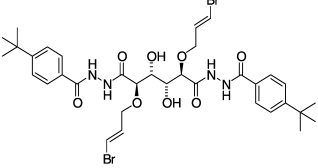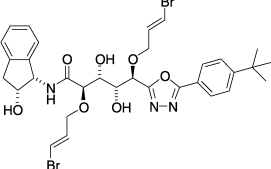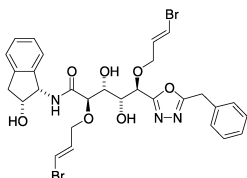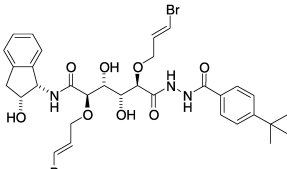
Compound	Structure	ΔG_{bind} (kcal/mol)			
		Plm II		Plm IV	
		experimental[1]	LIE[2]	experimental[1]	LIE[3]
18		−8.8	−9.4 ± 1.2	−7.1	−4.9 ± 0.7
19		−9.5	−9.1 ± 0.8	−9.2	−9.9 ± 1.3
20		−8.2	−7.6 ± 1.4	−7.8	−7.6 ± 1.6
21		−7.3	−7.6 ± 1.0	−7.8	−8.0 ± 0.6
22		−8.7	−9.5 ± 0.2	−10.2	−9.9 ± 0.3
23		−8.0	−	−8.7	−9.2 ± 0.4
24		n.d.	−	−8.1	−7.4 ± 0.5

Table 1 *(Continued)*

Compound	Structure	ΔG_{bind} (kcal/mol)			
		Plm II		Plm IV	
		experimental[1]	LIE[2]	experimental[1]	LIE[3]
25		−7.8	–	−7.8	−8.7 ± 0.5
26		−9.4	–	−6.7	−6.5 ± 0.4

[1] Free energies of binding were obtained from experimental affinity values with the equation $\Delta G = RT \ln K_i$.
[2] Error estimates were obtained by comparing average values from the first and second half of the MD sampling.
[3] Average binding free energies from the Plm IV homology model and 1LS5 structures (the combined LIE model) [54]; for the macrocyclic compounds **18–21**, only the 1LS5 structure was used for calculations [16].
[4] Asterisks (*) denote the stereocentra, [see ref. 23 for details].
[5] Calculated value is for the charged compound.

static contributions for the two compounds were of equal magnitude, despite the fact that the number of hydrogen bond donors and acceptors was decreased. Thus, the hydrogen bond donors/acceptors of **1** do not effectively contribute to the binding affinity as they are equally well solvated in the enzyme and in solution.

In the next phase, the inhibitor side chains in the P1/P1′ position were optimized. Allyloxy was exchanged by benzyloxy (**4**), or extended by different aromatic systems (**6–9**) in the parent compound **3** [51]. The extension (4-acetylphenyl group) present in compound **7** was predicted to be the best substitution, in agreement with experimental results. In fact, compound **7** displayed 78% inhibition of parasite growth at 5 μM. The other substitutions (**4**, **6**, **8**, **9**) resulted in improved binding energies in comparison to the parent compound **3**, but not to the same extent as **7**. When the calculated interaction energies for these compounds were evaluated, the observed trend was that the major contribution to the binding free energy was due to nonpolar interactions, while the electrostatic component was generally small and not always favorable. The linkers in the P1/P1′ substituents were extended compared to the benzyloxy and allyloxy side chains of **3** and **4**, but were nonetheless well accommodated in both the S1 and the S1′ binding pockets. The P1 extension was aligned along S1–S3, thus displacing the indanol moiety towards the S2 pocket. The S1′ subsite was shown to be more flexible, allowing the P1′ of the inhibitor to reach through it

towards the solvent. This led to the conclusion that, theoretically, there is no limit to the length of the P1′ side chain.

In an attempt to modify the scaffold, the amide linker between the P1 and P2 side chains in **3** was modified to methylamine, **5** (Table 1). In this way, the amine of the inhibitor would be protonated to a greater extent in the acidic food vacuole compared to the cytosol. The protonation of the amine could potentially trap the inhibitor in the food vacuole, as it would not be able to cross the vacuole membrane into the cytosol. This should result in a higher concentration of the drug in the organelle containing the target enzyme. Unfortunately, the inhibitor lost its activity, and from MD simulations it was concluded that this was related to the poor stabilization of the positive amine in the active site when compared to solution. The inhibitor was assumed to be charged in solution, but in the enzyme, both the charged and uncharged forms were considered. The protonated form resulted in better binding energy than the unprotonated one, but the enzyme was not able to stabilize the charge sufficiently. In principle, the positive charge of **5** should interact with the negatively charged catalytic aspartate (Asp214 in Plm II), mimicking the transiently protonated amine present during the peptide cleavage. According to our calculations, the amine of compound **5** was, however, located 5 Å away from Asp214, which is clearly not enough for stabilization of the charge. It should be noted, however, that even though compound **5** was ineffective against Plm I and Plm II, both
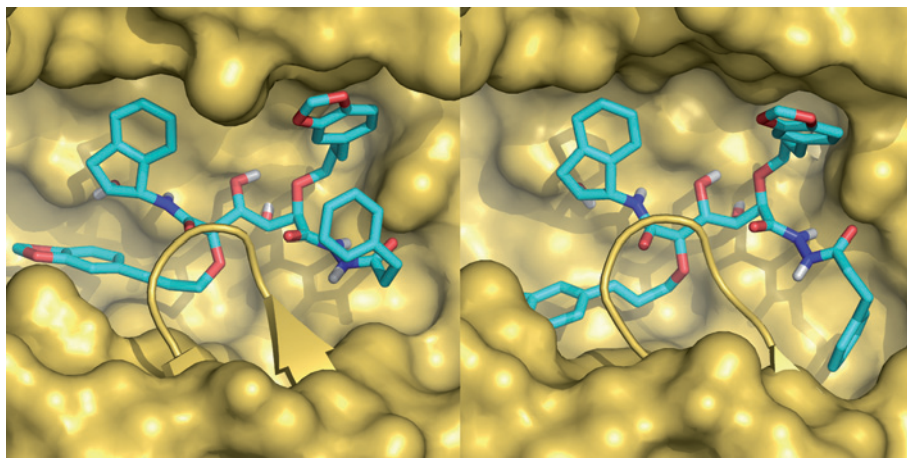
Figure 7. Compound **13** in two different conformations in the 1SME structure of Plm II. On the left side is shown the starting conformation of the MD simulation. On the right side is a snapshot of the MD simulation where the S2′ pocket has opened up to accommodate the large P2′ substituent.

by computational predictions and in *in vitro* assays, it was still found to inhibit parasite growth in cells by 50 % at 5 µM. Thus, **5** displayed activity almost in line with the best Plm II inhibitor but the mechanism of action was not resolved.

The compounds discussed so far (**1–9**) are peptide mimetics. The approach of using substrate-like compounds for inhibitor design is often very successful when it comes to finding potent inhibitors. However, for a compound to be useful as a drug, it requires not only reasonable affinity to the receptor, but also promising properties concerning absorption, delivery, metabolization and excretion (ADME). The ADME profiles for peptide mimetics are generally poor due to the proteolytic action of host enzymes. Consequently, we aimed to substitute one or both amide bonds in the previously designed inhibitors with one of two selected bioisosteres, diacylhydrazine or 1,3,4-oxadiazole.

Seven compounds comprising one of the two amide bond replacements were investigated through docking and LIE calculations [52]. A consequence of introducing the amide bond bioisosteres is that the C_2-symmetry of the compounds in the series is broken. Hence, two binding orientations had to be considered for each compound, to find the most favorable binding mode. These were compared with LIE calculations but did not initially show any significant preference for any of the binding modes. However, in the MD simulations, we observed considerable flexibility of the S2′ pocket, mainly originating from movements in the side chain of one amino acid (Met75). According to the simulations, when the pocket was widened compared to the initial crystal structure, the flexible phenylethyl sidechain (P2′ in **13**) was able to fit in the pocket. Once the phenyl ring was accommodated in the S2′ pocket, the simulation was extremely stable. The enlargement of the S2′ pocket and the insertion of the aromatic moiety reproduced an induced fit event, where the phenylethyl docked to the open S2′ and

locked it in that conformation. The flexibility of the S2′ pocket was confirmed in subsequent crystal structures (*e.g.* 1LF2 vs 1SME) [85, 88], where a 180° rotation of the Met75 side chain could indeed be observed. The rotation of the Met75 side chain in 1LF2 resulted in a large expansion of the S2′ pocket to accommodate the bulky P2′ moiety of the co-crystallized inhibitor in 1LF2. Our simulations with the bioisostere compounds were rerun, starting from the conformation with the expanded S2′ pocket. The new simulations yielded consistently stronger binding affinities for the binding mode with the bioisostere on the prime side. We therefore concluded a consensus binding mode for the new asymmetrical ligands in Plm II. In addition, the calculated binding affinities showed excellent correlation with experimental binding data. The predicted conformation of the potent compound **13** is shown in Figure 7, illustrating the induced fit of the S2′ pocket.

Subsequently, the impact of cyclization was investigated in four compounds (**18–21** in Table 1) [16]. The general idea of cyclization is to preorganize the ligand in a bioactive conformation thereby reducing the entropy loss upon binding [89]. Further benefits of cyclization are protection of the amide bonds from proteolytic cleavage and improved cell permeability [90]. Due to the structural difference of compounds **18–21** compared to our previous ligands and to any of the available co-crystallized inhibitors with Plm II [82, 85, 86], automated docking was performed to identify the binding mode of the new ligand structures (see Theoretical methods section below). The more constrained cyclic scaffold made it possible to find consensus docking solutions, in contrast to the linear compounds where the high flexibility made docking extremely difficult.

MD simulations and LIE calculations were carried out in both Plm II and Plm IV (1LS5 [O. A. Asoja, S. Gulnik, E. Afonina, R. Randad and A. Silva, unpub-
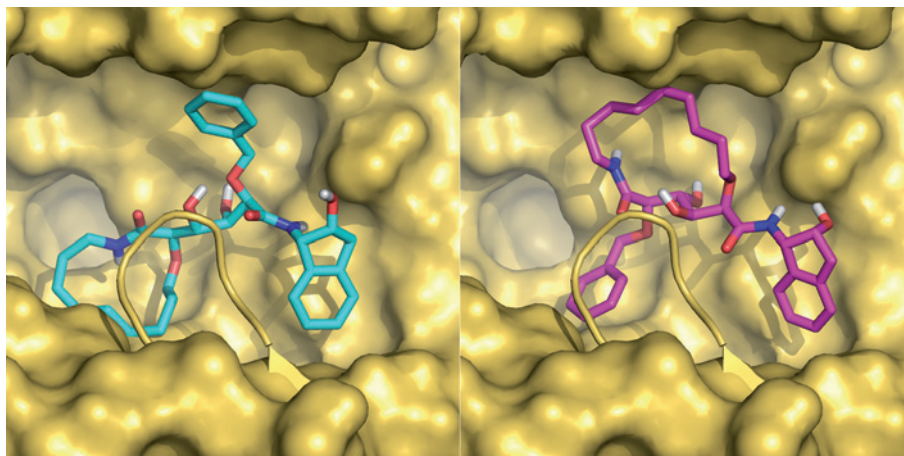
Figure 8. Macrocyclic inhibitors **19** (cyan) and **21** (magenta) docked to Plm II. The surface representation of the flap has been replaced with a cartoon for clarity. The 40-fold affinity difference between **19** and **21** can be explained by the conformations of the rings. The 13-membered ring of **19** fits perfectly in the S1-S3 subsite, whereas the 16-membered ring of **21** spans from S2 to P1′ and forces the central hydroxyl groups into unfavorable conformations.

lished data]), enabling us to elucidate the mechanisms of selectivity by deriving important differences in interaction patterns. The docking poses resulted in well-defined binding modes for the four compounds in Plm II. In Plm IV, there emerged a number of plausible binding modes, but from MD simulations we could conclude that only the docking solutions consistent with the Plm II solutions were stable during simulations. The result is in agreement with the general hypothesis of a conserved binding mode among different plasmepsins [91, 92]. In contrast to the binding mode identified for previous asymmetric inhibitors, the amino indanol fragment was placed in the S2′ pocket in all cases. The conformations of the macrocycles depended on their size; the 13-membered ring of **18** and **19** was docked in the S1–S3 cleft, while the 16-membered ring of **20** and **21** fitted in the S2 site (Fig. 8). For **20** and **21**, the transition state mimicking hydroxyl groups were forced to point in opposite directions, with only one of them able to form hydrogen bonds with the catalytic aspartates. These conformations give a plausible explanation for the lower affinity of these compounds. The excellent agreement between calculated and experimental affinities for the four compounds in the two enzymes (see Table 1) provided a strong argument for the reliability of the predicted binding modes [16].

Analysis of the MD simulations showed that the different experimental affinities observed between **18** and **19** in Plm IV originated from differences in the electrostatic interaction between the active site aspartates and the two hydroxyl groups in the transition state mimic core [16]. The introduction of the double bond in the macrocycle produced a constrained conformation of the cycle in the S1–S3 pocket for **18**. This in turn caused a shift of the ligand, thereby disrupting the important hydrogen bond pattern of the transition state mimic hydroxyl. This pattern was not observed in the more open S1–S3

pocket of Plm II, which explains the experimental equipotency measured for **18** and **19** in Plm II. This example clearly demonstrates the use of MD simulations for predicting selectivity of an inhibitor towards related enzymes.

Inhibitor binding to Plm IV: influence of the protein structure

To further examine the mechanism of selectivity between different plasmepsins, nine more compounds were selected for computational studies in Plm IV (see Table 1) [54]. This set of inhibitors offered large chemical diversity in the P2 and P2′ side chains and displayed a broad spectrum of experimental inhibitory activities against Plm IV. Two different protein models were used, the crystal structure 1LS5 [O. A. Asojo et al., unpublished data] and a homology model. The homology model of Plm IV was built to complement the low resolution (and unpublished) crystal structure and, in addition, enabled a comparison of affinity predictions using two different structural models of the same enzyme.

Four templates available in the PDB were used to create the homology model: three structures of Plm II (1LF2, 1LEE [85] and 1M43 [86]) and Plm IV from *P. vivax* (1QS8) [93]. Information about protein flexibility was implicitly included into the protein model structure through the use of various templates that possess structural differences. One example of the usefulness of this approach is the docking performed with the homology model. When the 1LS5 structure was used as protein model in the docking, no consensus binding orientation could be identified for the asymmetrical inhibitors (compounds **12, 13, 16, 17, 24–26**). However, when the same dockings were repeated with the homology model, the same binding orientation as previously described for Plm II [52] was

easily identified. Thus, the flexibility of the protein was to some extent incorporated into the homology model.

The differences between the homology model and the crystal structure were also assessed in MD/LIE calculations. Reasonable agreement was achieved between calculated and experimental binding affinities with both models. Remarkably, however, a significant improvement in the root mean square errors of the predictions was obtained when the energetic data of the two structures were combined ('combined LIE model', see Table 1 and Fig. 9). This gave a satisfactory answer to the question of dependence of the LIE results on the initial protein geometry, leading to the conclusion that different starting points can, in fact, improve the statistical sampling and consequently the predictive power of the method [54].
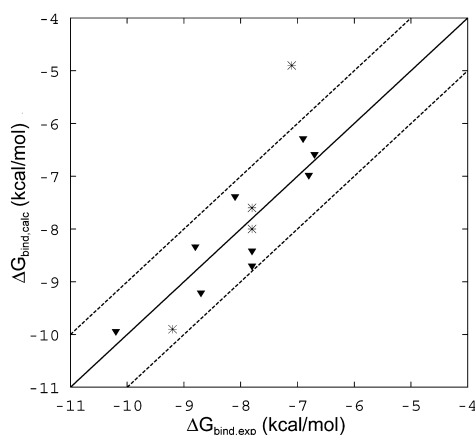

Figure 9. The combined LIE model, with binding energies calculated both from the Plm IV crystal structure and the homology model, reproduces the experimental binding energies very well (triangles). The asterisks correspond to the macrocyclic compounds only simulated in the 1LS5 crystal structure.

A detailed analysis of the MD simulations followed, in order to rationalize the binding characteristics of the inhibitor series in Plm IV. The most potent Plm IV inhibitor in the series (**22**) was selective toward Plm IV over Plm II. This selectivity was explained by the shape complementarity of the S2/S2′ substitution to their respective subsites, thereby anchoring the inhibitor in the binding site, and thus supporting the interactions with the catalytic residues. In contrast to what was observed in Plm II simulations, the S2′ site always remained rigid during the MD simulations. The presence of a rigid Ile in position 75 of Plm IV, instead of the flexible Met in Plm II, was identified as the source of the different dynamic behavior of the two enzymes. This was also the structural basis for the interpretation of the decreased activity observed for compounds with a bulky P2′ sidechain (**12**, **13**) with

respect to Plm II. Thus, not only the structural rationale for affinity but also for selectivity between two closely related enzymes (Plm II and Plm IV) could be addressed with our computational strategy.

In all of the discussed calculations on reaction profiles and Plm II and IV inhibitors, the protonation state of the catalytic aspartates with Asp34 protonated has been found to yield consistent results. However, we recently also carried out simulations of Plm IV complexes with a class of allophenylnorstatin inhibitors after a crystal structure in complex with *P. malariae* Plm IV had been published [94]. These calculations surprisingly showed that in this case it is Asp214 that instead is protonated [55]. This demonstrates that it is essential to consider the possibility of different protonation states for different classes of inhibitor.

Are scoring functions reliable for binding energy prediction?

In addition to the LIE method, the use of scoring functions was evaluated within the present project. The Chemscore scoring function of Eldrige et al. [35] was initially found not to yield a correct ranking of the different stereoisomers [23]. That is, scoring of single minimized complexes between the enzyme and the inhibitor resulted in energies that scored the allyloxy stereoisomers incorrectly (**1**). On the other hand the scoring function performed satisfactorily using the same methodology on the benzyloxy stereoisomers (**2**). By averaging the score over 100 snapshots, the scoring function managed to rank the isomer series according to their binding affinity. Taking a single complex demonstrates how vulnerable the scoring functions are to choosing an inhibitor conformation that is not representative of the available conformational ensemble. On the other hand, scoring single structures of course has the advantage of reducing computational costs considerably. The X-score scoring function [36] was used to examine the simulations of Plm IV with the linear compounds (binding free energies for **12, 13, 16, 17, 22–26** are presented in Fig. 10a). A good agreement with experimental results was again obtained when we considered average scores obtained from the MD snapshots. It is, however, worth noting that in most cases, significant differences existed between mean scoring values obtained by MD sampling and the scoring of the static initial pose (Fig. 10b). This indicates that thermal conformational sampling by MD simulations, although time consuming, can be used for improving the accuracy of empirical scores.
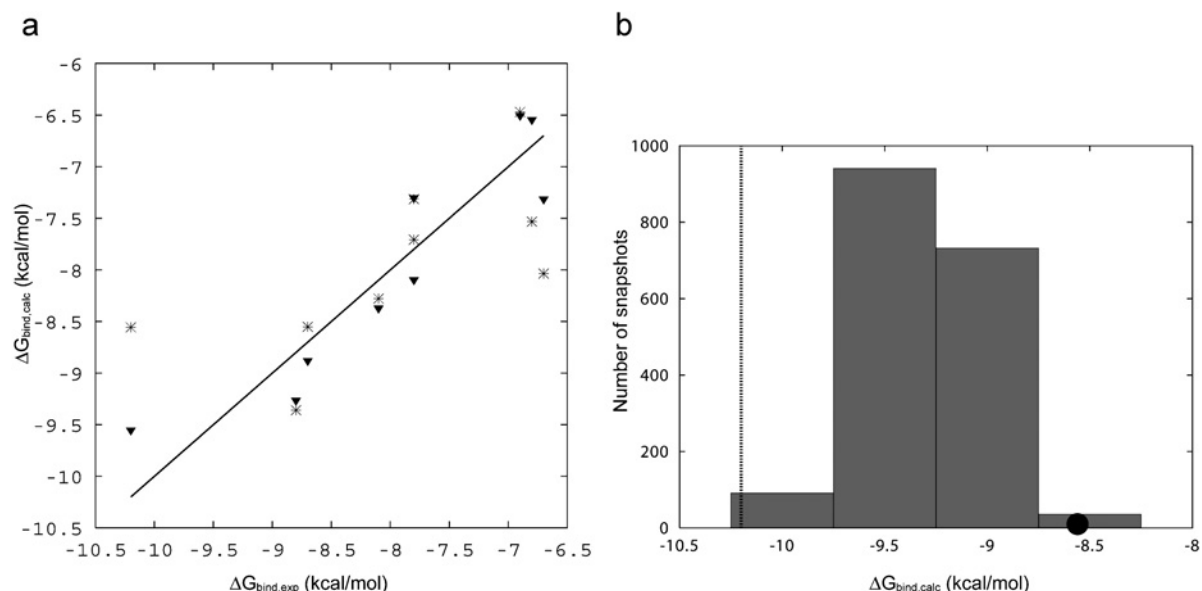
Figure 10. Scatter plot for calculated versus experimental free energies of binding for Plm IV inhibitors, using the X-score function (left). Triangles correspond to average values from MD simulations, while asterisks depict the score of the initial docking pose. Separate regression constants were added to the two series. The right panel illustrates the effect of conformational sampling on the scoring for ligand **22**. The black dot represents the score from the single conformation score, and the histogram displays the distribution of scores for MD snapshots. The experimental value is represented by a vertical dotted line.

Concluding remarks

The 1,2-dihydroxyethylene-based inhibitors reported in Table 1 are the result of successful efforts to generate new lead compounds that inhibit the growth of *P. falciparum* [16, 23, 51, 52]. These inhibitors were designed to obstruct the function of plasmepsins that are part of the catabolic pathway in the parasite. The effectiveness of the inhibitors was supported by experiments on cells, where 78% inhibition of parasite growth rate in red blood cells was achieved for the most potent inhibitor, **7**. Furthermore, none of the discussed inhibitors interfere with human cathepsin D, which is rather unique and makes them particularly interesting for further development. The approach of combining computational techniques with organic synthesis was shown to be useful in delivering highly potent inhibitors and in providing directions for further improvements. The affinities of this series of ligands were evaluated and supported by both experimental and theoretical techniques. The strength of combining experimental and theoretical techniques is also, *e.g.* illustrated by the fact that the affinity was remeasured for two compounds due to large differences from the predicted values, resulting in reevaluated experimental binding affinities in better accord with the calculated ones. In conclusion, the discussed efforts in designing new inhibitors against malarial plasmepsins very clearly demonstrate the effectiveness of employing a range of computational tools in the design process, including homology modeling, automated docking, enzyme reaction simulations and microscopic calculations of binding free energies.

Theoretical methods

The LIE method
Absolute binding free energies were determined by the LIE method [40] for the investigated Plm II and Plm IV inhibitors **1–26** [16, 23, 51, 52]. The LIE method employs MD simulation averaging of the intermolecular interactions between the ligand and its surrounding environment in the two relevant states, *i.e.* the ligand solvated in water (free state) and the solvated protein–ligand complex (bound state). MD sampling of the protein–ligand complex allows structural and energetic relaxation of the starting structures. This is a major difference compared to the use of scoring functions, where binding energy is usually determined from a single energy minimized receptor/ligand complex. Prior to all simulations, the ligand or the ligand–protein complex was solvated with explicit water molecules, and restrained spherical simulation boundaries were used in all calculations. Further details regarding the MD simulation protocols can be found in the original papers [16, 23, 51, 52].
The electrostatic (el) and van der Waals (vdW) potential energies of the ligand with its surroundings are collected from the simulations. The difference for

each potential energy contribution (U^{el} or U^{vdW}), between the bound and free states is determined and translated into the corresponding polar and nonpolar components of the binding free energy (ΔG^{polar} and $\Delta G^{nonpolar}$), through the use of the electrostatic linear response approximation and an empirical correlation between the van der Waals energies and the hydrophobic (nonpolar) contribution [40, 95, 96]. The LIE equation is written as

$$
\Delta G_{bind} = \alpha \left(\langle U_{l-s}^{vdw} \rangle_{bound} - \langle U_{l-s}^{vdw} \rangle_{free} \right) \\
+ \beta \left(\langle U_{l-s}^{el} \rangle_{bound} - \langle U_{l-s}^{el} \rangle_{free} \right) + \gamma \tag{1}
$$

where $\langle \cdot \rangle$ denotes an ensemble average of intermolecular interactions between the ligand (l) and surrounding (s) for the bound and free state. The parameters α and β are empirically and theoretically derived, respectively [40, 95, 96]. Furthermore, all Plm II calculations yield a good correlation between calculated and estimated affinities with no constant term (γ) added (Fig. 11). In the Plm IV system, however, there was a tendency to underestimate the absolute free energies of binding, and the addition of a nonzero γ improved the results.
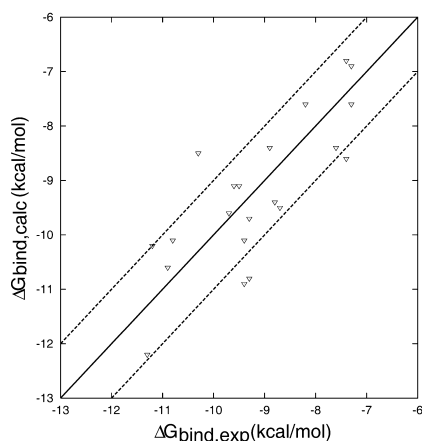

Figure 11. Calculated binding free energies reproduce very well the experimentally determined values for Plm II inhibitors [16, 23, 51, 52]. Dashed lines denote a 1 kcal/mol mark.

Docking
Manual docking and automated docking with Auto-Dock3 [27] or GOLD2.2 [32] were used to obtain starting inhibitor conformations necessary for the molecular dynamics simulations. Manual docking was performed on the linear compounds (**1–17**) by superimposing the central part of the compounds onto the corresponding part of pepstatin A (1SME [88]). Here, it is initially assumed that the hydrogen bond network

is conserved for the backbone of the ligands. The side chains of the ligands were then fitted to each corresponding subsite to minimize steric clashes. The first part of the equilibration phase in the MD simulations corresponds to a minimization procedure, and relaxes ligand-protein strain. In the studies involving Plm IV [54] and the macrocyclic inhibitors **18–21** of Plm II [16] GOLD2.2 [32] was employed. Both the Goldscore and Chemscore functions of GOLD2.2 were utilized in parallel docking runs. To capture the flexible nature of the plasmepsins, we used multiple protein models (1LF2 and 1LF3 for Plm II [85]; 1LS5 [91] and a homology model for Plm IV).

Scoring
Two empirical scoring functions were used to predict the inhibitor binding affinity and ranking. The Chemscore scoring function [35] was used initially to select the most potent stereoisomer [23]. It consists of five different terms that account for hydrogen bonding, interactions with metal ions, lipophilic interactions and the number of rotatable bonds, each consisting of an empirical constant (ΔG_x) that multiplies the number of occurrences:

$$
\Delta G_{bind} = \Delta G_{H-bond} N_{H-bond} \\
+ \Delta G_{metal} N_{metal} + \Delta G_{lipo} N_{lipo} \\
+ \Delta G_{rot} N_{rot} + \Delta G_0 \tag{2}
$$

In addition the X-score function [36]

$$
\Delta G_{bind} = \Delta G_{vdW} + \Delta G_{H-bond} \\
+ \Delta G_{rot} + \Delta G_{hydrophobic} + \Delta G_0 \tag{3}
$$

was employed in the characterization of the Plm-IV-binding site [54]. In eq. 3, ΔG_{vdW} accounts for the van der Waals energy between ligand and protein and ΔG_{H-bond} is a hydrogen bond term. The hydrophobic effect ($\Delta G_{hydrophobic}$) is calculated as a combination of three different algorithms (named hydrophobic contact, hydrophobic surface and hydrophobic matching). The term ΔG_{rot} accounts for the rotational entropy of the ligand.

1 Snow, R. W., Guerra, C. A., Noor, A. M., Myint, H. Y., and Hay, S. I. (2005) The global distribution of clinical episodes of *Plasmodium falciparum* malaria. Nature 434, 214 – 217.
2 Baird, J. K. (2005) Drug therapy: effectiveness of antimalarial drugs. N. Engl. J. Med. 352, 1565 – 1577.

3 Targett, G. A. (2005) Malaria vaccines 1985 – 2005: a full circle? Trends Parasitol. 21, 499 – 503.

4 Greenwood, B., and Mutabingwa, T. (2002) Malaria in 2002. Nature 415, 670 – 672.

5 Greenwood, B. (2005) Malaria vaccines evaluation and implementation. Acta Trop. 95, 298 – 304.

6 Greenwood, B. M., Bojang, K., Whitty, C. J. M., and Targett, G. A. T. (2005) Malaria. Lancet 365, 1487 – 1498.

7 Miller, L. H., Baruch, D. I., Marsh, K., and Doumbo, O. K. (2002) The pathogenic basis of malaria. Nature 415, 673 – 679.

8 Alonso, P. L., Sacarlal, J., Aponte, J. J., Leach, A., Macete, E., Milman, J., Mandomando, I., Spiessens, B., Guinovart, C., Espasa, M., Bassat, Q., Aide, P., Ofori-Anyinam, O., Navia, M. M., Corachan, S., Ceuppens, M., Dubois, M. C., Demoitie, M. A., Dubovsky, F., Menendez, C., Tornieporth, N., Ballou, W. R., Thompson, R., and Cohen, J. (2004) Efficacy of the RTS,S/ AS02A vaccine against *Plasmodium falciparum* infection and disease in young African children: randomised controlled trial. Lancet 364, 1411 – 1420.

9 Alonso, P. L., Sacarlal, J., Aponte, J. J., Leach, A., Macete, E., Aide, P., Sigauque, B., Milman, J., Mandomando, I., Bassat, Q., Guinovart, C., Espasa, M., Corachan, S., Lievens, M., Navia, M. M., Dubois, M. C., Menendez, C., Dubovsky, F., Cohen, J., Thompson, R., and Ballou, W. R. (2005) Duration of protection with RTS,S/AS02A malaria vaccine in prevention of *Plasmodium falciparum* disease in Mozambican children: single-blind extended follow-up of a randomised controlled trial. Lancet 366, 2012 – 2018.

10 Biagini, G. A., Viriyavejakul, P., O'Neill, P. M., Bray, P. G., and Ward, S. A. (2006) Functional characterization and target validation of alternative complex I of *Plasmodium falciparum* mitochondria. Antimicrob. Agents Chemother. 50, 1841 – 1851.

11 Mi-Ichi, F., Miyadera, H., Kobayashi, T., Takamiya, S., Waki, S., Iwata, S., Shibata, S., and Kita, K. (2005) Parasite mitochondria as a target of chemotherapy – inhibitory effect of licochalcone A on the *Plasmodium falciparum* respiratory chain. In: Natural Products and Molecular Therapy (Kotwal, G. J. and Lahiri, D. K., Eds.), pp 46 – 54, New York Academy of Sciences, New York.

12 Beitz, E. (2005) Aquaporins from pathogenic protozoan parasites: structure, function and potential for chemotherapy. Biol. Cell 97, 373 – 383.

13 Reguera, R. M., Tekwani, B. L., and Balana-Fouce, R. (2005) Polyamine transport in parasites: a potential target for new antiparasitic drug development. Comp. Biochem. Physiol. C Comp. Pharmacol. Toxicol. 140, 151 – 164.

14 Eastman, R. T., Buckner, F. S., Yokoyama, K., Gelb, M. H., and Van Voorhis, W. C. (2006) Fighting parasitic disease by blocking protein farnesylation. J. Lipid Res. 47, 233 – 240.

15 Coppi, A., Cabinian, M., Mirelman, D., and Sinnis, P. (2006) Antimalarial activity of allicin, a biologically active compound from garlic cloves. Antimicrob. Agents Chemother. 50, 1731 – 1737.

16 Ersmark, K., Nervall, M., Gutierrez-de-Teran, H., Hamelink, E., Janka, L. K., Clemente, J. C., Dunn, B. M., Gogoll, A., Samuelsson, B., Åqvist, J., and Hallberg, A. (2006) Macrocyclic inhibitors of the malarial aspartic proteases plasmepsin I, II, and IV. Bioorg. Med. Chem. 14, 2197 – 2208.

17 Micale, N., Kozikowski, A. P., Ettari, R., Grasso, S., Zappala, M., Jeong, J. J., Kumar, A., Hanspal, M., and Chishti, A. H. (2006) Novel peptidomimetic cysteine protease inhibitors as potential antimalarial agents. J. Med. Chem. 49, 3064 – 3067.

18 Yanow, S. K., Purcell, L. A., and Spithill, T. W. (2006) The A/T-specific DNA alkylating agent adozelesin inhibits *Plasmodium falciparum* growth in vitro and protects mice against *Plasmodium chabaudi adami* infection. Mol. Biochem. Parasitol. 148, 52 – 59.

19 Goldberg, D. E., Slater, A. F., Beavis, R., Chait, B., Cerami, A., and Henderson, G. B. (1991) Hemoglobin degradation in the human malaria pathogen *Plasmodium falciparum*: a catabolic pathway initiated by a specific aspartic protease. J. Exp. Med. 173, 961 – 9.

20 Liu, J., Gluzman, I. Y., Drew, M. E., and Goldberg, D. E. (2005) The role of *Plasmodium falciparum* food vacuole plasmepsins. J. Biol. Chem. 280, 1432 – 1437.

21 Omara-Opyene, A. L., Moura, P. A., Sulsona, C. R., Bonilla, J. A., Yowell, C. A., Fujioka, H., Fidock, D. A., and Dame, J. B. (2004) Genetic disruption of the *Plasmodium falciparum* digestive vacuole plasmepsins demonstrates their functional redundancy. J. Biol. Chem. 279, 54088 – 54096.

22 Liu, J., Istvan, E. S., Gluzman, I. Y., Gross, J., and Goldberg, D. E. (2006) *Plasmodium falciparum* ensures its amino acid supply with multiple acquisition pathways and redundant proteolytic enzyme systems. Proc. Natl. Acad. Sci. USA. 103, 8840 – 8845.

23 Ersmark, K., Feierberg, I., Bjelic, S., Hulten, J., Samuelsson, B., Åqvist, J., and Hallberg, A. (2003) C_2-symmetric inhibitors of *Plasmodium falciparum* plasmepsin II: synthesis and theoretical predictions. Bioorg. Med. Chem. 11, 3723 – 3733.

24 Nezami, A., Luque, I., Kimura, T., Kiso, Y., and Freire, E. (2002) Identification and characterization of allophenylnorstatine-based inhibitors of plasmepsin II, an antimalarial target. Biochemistry 41, 2273 – 2280.

25 Gohlke, H., and Klebe, G. (2002) Approaches to the description and prediction of the binding affinity of small-molecule ligands to macromolecular receptors. Angew. Chem. Int. Ed. 41, 2645 – 2676.

26 Jorgensen, W. L. (2004) The many roles of computation in drug discovery. Science 303, 1813 – 1818.

27 Morris, G. M., Goodsell, D. S., Halliday, R. S., Huey, R., Hart, W. E., Belew, R. K., and Olson, A. J. (1998) Automated docking using a Lamarckian genetic algorithm and an empirical binding free energy function. J. Comput. Chem. 19, 1639 – 1662.

28 Ewing, T. J. A., and Kuntz, I. D. (1997) Critical evaluation of search algorithms for automated molecular docking and database screening. J. Comput. Chem. 18, 1175 – 1189.

29 Rarey, M., Kramer, B., Lengauer, T., and Klebe, G. (1996) A fast flexible docking method using an incremental construction algorithm. J. Mol. Biol. 261, 470 – 489.

30 Friesner, R. A., Banks, J. L., Murphy, R. B., Halgren, T. A., Klicic, J. J., Mainz, D. T., Repasky, M. P., Knoll, E. H., Shelley, M., Perry, J. K., Shaw, D. E., Francis, P., and Shenkin, P. S. (2004) Glide: a new approach for rapid, accurate docking and scoring. 1. Method and assessment of docking accuracy. J. Med. Chem. 47, 1739 – 1749.

31 Halgren, T. A., Murphy, R. B., Friesner, R. A., Beard, H. S., Frye, L. L., Pollard, W. T., and Banks, J. L. (2004) Glide: a new approach for rapid, accurate docking and scoring. 2. Enrichment factors in database screening. J. Med. Chem. 47, 1750 – 1759.

32 Jones, G., Willett, P., Glen, R. C., Leach, A. R., and Taylor, R. (1997) Development and validation of a genetic algorithm for flexible docking. J. Mol. Biol. 267, 727 – 748.

33 Verdonk, M. L., Cole, J. C., Hartshorn, M. J., Murray, C. W., and Taylor, R. D. (2003) Improved protein-ligand docking using GOLD. Proteins Struct. Funct. Genet. 52, 609 – 623.

34 Wang, R. X., Lu, Y. P., Fang, X. L., and Wang, S. M. (2004) An extensive test of 14 scoring functions using the PDBbind refined set of 800 protein-ligand complexes. J. Chem. Inf. Comput. Sci. 44, 2114 – 2125.

35 Eldridge, M. D., Murray, C. W., Auton, T. R., Paolini, G. V., and Mee, R. P. (1997) Empirical scoring functions. 1. The development of a fast empirical scoring function to estimate the binding affinity of ligands in receptor complexes. J. Comput. Aided Mol. Des. 11, 425 – 445.

36 Wang, R. X., Lai, L. H., and Wang, S. M. (2002) Further development and validation of empirical scoring functions for structure-based binding affinity prediction. J. Comput. Aided Mol. Des. 16, 11 – 26.

37 Velec, H. F. G., Gohlke, H., and Klebe, G. (2005) DrugScore(CSD)-knowledge-based scoring function derived from small molecule crystal data with superior recognition rate of near-

native ligand poses and better affinity prediction. J. Med. Chem. 48, 6296 – 6303.

38 Brandsdal, B. O., Österberg, F., Almlöf, M., Feierberg, I., Luzhkov, V. B., and Åqvist, J. (2003) Free energy calculations and ligand binding. Adv. Protein Chem. 66, 123 – 158.

39 Luzhkov, V. B., and Åqvist, J. (2001) Mechanisms of tetraethylammonium ion block in the KcsA potassium channel. FEBS Lett. 495, 191 – 6.

40 Åqvist, J., Medina, C., and Samuelsson, J. E. (1994) New method for predicting binding affinity in computer-aided drug design. Protein Eng. 7, 385 – 391.

41 Åqvist, J., and Marelius, J. (2001) The linear interaction energy method for predicting ligand binding free energies. Comb. Chem. High Throughput Screen. 4, 613 – 626.

42 Åqvist, J., Luzhkov, V. B., and Brandsdal, B. O. (2002) Ligand binding affinities from MD simulations. Acc. Chem. Res. 35, 358 – 365.

43 Huang, D., and Caflisch, A. (2004) Efficient evaluation of binding free energy using continuum electrostatics solvation. J. Med. Chem. 47, 5791 – 5797.

44 Tominaga, Y., and Jorgensen, W. L. (2004) General model for estimation of the inhibition of protein kinases using Monte Carlo simulations. J. Med. Chem. 47, 2534 – 2549.

45 Zhou, R. H., Friesner, R. A., Ghosh, A., Rizzo, R. C., Jorgensen, W. L., and Levy, R. M. (2001) New linear interaction method for binding affinity calculations using a continuum solvent model. J. Phys. Chem. B 105, 10388 – 10397.

46 Zoete, V., Michielin, O., and Karplus, M. (2003) Protein-ligand binding free energy estimation using molecular mechanics and continuum electrostatics: application to HIV-1 protease inhibitors. J. Comput. Aided Mol. Des. 17, 861 – 880.

47 Lee, F. S., Chu, Z. T., Bolger, M. B., and Warshel, A. (1992) Calculations of antibody-antigen interactions: microscopic and semi-microscopic evaluation of the free energies of binding of phosphorylcholine analogs to McPC603. Protein Eng. 5, 215 – 228.

48 Sham, Y., Chu, Z. T., Tao, H., and Warshel, A. (2000) Examining methods for calculations of binding free energies: LRA, LIE, PDLD-LRA and PDLD/S-LRA calculations of ligands binding to an HIV protease. Proteins 39, 393 – 407.

49 Kollman, P. A., Massova, I., Reyes, C., Kuhn, B., Huo, S. H., Chong, L., Lee, M., Lee, T., Duan, Y., Wang, W., Donini, O., Cieplak, P., Srinivasan, J., Case, D. A., and Cheatham, T. E. (2000) Calculating structures and free energies of complex molecules: combining molecular mechanics and continuum models. Acc. Chem. Res. 33, 889 – 897.

50 Carlsson, J., and Åqvist, J. (2006) Calculations of solute and solvent entropies from molecular dynamics simulations. Phys. Chem. Chem. Phys. 8, 5385 – 5395.

51 Ersmark, K., Feierberg, I., Bjelic, S., Hamelink, E., Hackett, F., Blackman, M. J., Hulten, J., Samuelsson, B., Åqvist, J., and Hallberg, A. (2004) Potent inhibitors of the *Plasmodium falciparum* enzymes plasmepsin I and II devoid of cathepsin D inhibitory activity. J. Med. Chem. 47, 110 – 122.

52 Ersmark, K., Nervall, M., Hamelink, E., Janka, L. K., Clemente, J. C., Dunn, B. M., Blackman, M. J., Samuelsson, B., Åqvist, J., and Hallberg, A. (2005) Synthesis of malarial plasmepsin inhibitors and prediction of binding modes by molecular dynamics simulations. J. Med. Chem. 48, 6090 – 6106.

53 Ersmark, K., Samuelsson, B., and Hallberg, A. (2006) Plasmepsins as potential targets for new antimalarial therapy. Med. Res. Rev. 26, 626 – 666.

54 Gutiérrez-de-Terán, H., Nervall, M., Ersmark, K., Dunn, B. M., Hallberg, A., and Åqvist, J. (2006) Inhibitor binding to the plasmepsin IV aspartic protease from *Plasmodium falciparum*. Biochemistry 45, 10529 – 10541.

55 Gutiérrez-de-Terán, H., Nervall, M., Dunn, B. M., Clemente, J. C., and Åqvist, J. (2006) Computational analysis of plasmepsin IV bound to an allophenylnorstatine inhibitor. FEBS Lett. 580, 5910 – 5916.

56 Haque, T. S., Skillman, A. G., Lee, C. E., Habashita, H., Gluzman, I. Y., Ewing, T. J. A., Goldberg, D. E., Kuntz, I. D., and Ellman, J. A. (1999) Potent, low-molecular-weight non-peptide inhibitors of malarial aspartyl protease plasmepsin II. J. Med. Chem. 42, 1428 – 1440.

57 Graffner-Nordberg, M., Kolmodin, K., Åqvist, J., Queener, S. F., and Hallberg, A. (2004) Design, synthesis, and computational affinity prediction of ester soft drugs as inhibitors of dihydrofolate reductase from *Pneumocystis carinii*. Eur. J. Pharm. Sci. 22, 43 – 54.

58 Graffner-Nordberg, M., Kolmodin, K., Åqvist, J., Queener, S. F., and Hallberg, A. (2001) Design, synthesis, computational prediction, and biological evaluation of ester soft drugs as inhibitors of dihydrofolate reductase from *Pneumocystis carinii*. J. Med. Chem. 44, 2391 – 402.

59 Graffner-Nordberg, M., Marelius, J., Ohlsson, S., Persson, A., Swedberg, G., Andersson, P., Andersson, S. E., Åqvist, J., and Hallberg, A. (2000) Computational predictions of binding affinities to dihydrofolate reductase: synthesis and biological evaluation of methotrexate analogues. J. Med. Chem. 43, 3852 – 61.

60 Marelius, J., Graffner-Nordberg, M., Hansson, T., Hallberg, A., and Åqvist, J. (1998) Computation of affinity and selectivity: binding of 2,4-diaminopteridine and 2,4-diaminoquinazoline inhibitors to dihydrofolate reductases. J. Comput. Aided Drug Des. 12, 119 – 31.

61 Rizzo, R. C., Tirado-Rives, J., and Jorgensen, W. L. (2001) Estimation of binding affinities for HEPT and nevirapine analogues with HTV-1 reverse transcriptase via Monte Carlo simulations. J. Med. Chem. 44, 145 – 154.

62 Rizzo, R. C., Udier-Blagovic, M., Wang, D. P., Watkins, E. K., Smith, M. B. K., Smith, R. H., Tirado-Rives, J., and Jorgensen, W. L. (2002) Prediction of activity for nonnucleoside inhibitors with HIV-1 reverse transcriptase based on Monte Carlo simulations. J. Med. Chem. 45, 2970 – 2987.

63 Rizzo, R. C., Wang, D. P., Tirado-Rives, J., and Jorgensen, W. L. (2000) Validation of a model for the complex of HIV-1 reverse transcriptase with sustiva through computation of resistance profiles. J. Am. Chem. Soc. 122, 12898 – 12900.

64 Smith, R. H., Jorgensen, W. L., Tirado-Rives, J., Lamb, M. L., Janssen, P. A. J., Michejda, C. J., and Smith, M. B. K. (1998) Prediction of binding affinities for TIBO inhibitors of HIV-1 reverse transcriptase using Monte Carlo simulations in a linear response method. J. Med. Chem. 41, 5272 – 5286.

65 Huang, D. Z., Luthi, U., Kolb, P., Cecchini, M., Barberis, A., and Caflisch, A. (2006) In silico discovery of beta-secretase inhibitors. J. Am. Chem. Soc. 128, 5436 – 5443.

66 Huo, S., Wang, J., Cieplak, P., Kollman, P. A., and Kuntz, I. D. (2002) Molecular dynamics and free energy analyses of cathepsin D–inhibitor interactions: insight into structure-based ligand design. J. Med. Chem. 45, 1412 – 1419.

67 Srinivasan, J., Cheatham, T. E., Cieplak, P., Kollman, P. A., and Case, D. A. (1998) Continuum solvent studies of the stability of DNA, RNA, and phosphoramidate–DNA helices. J. Am. Chem. Soc. 120, 9401 – 9409.

68 Kuhn, B., and Kollman, P. A. (2000) Binding of a diverse set of ligands to avidin and streptavidin: an accurate quantitative prediction of their relative affinities by a combination of molecular mechanics and continuum solvent models. J. Med. Chem. 43, 3786 – 3791.

69 Becker, O. M., Dhanoa, D. S., Marantz, Y., Chen, D. L., Shacham, S., Cheruku, S., Heifetz, A., Mohanty, P., Fichman, M., Sharadendu, A., Nudelman, R., Kauffman, M., and Noiman, S. (2006) An integrated in silico 3D model-driven discovery of a novel, potent, and selective amidosulfonamide 5-HT1A agonist (PRX-00023) for the treatment of anxiety and depression. J. Med. Chem. 49, 3116 – 3135.

70 Bjelic, S., and Åqvist, J. (2004) Computational prediction of structure, substrate binding mode, mechanism, and rate for a malaria protease with a novel type of active site. Biochemistry 43, 14521 – 14528.

71 Bjelic, S., and Åqvist, J. (2006) Catalysis and linear free energy relationships in aspartic proteases. Biochemistry 45, 7709 – 7723.

72 Coombs, G. H., Goldberg, D. E., Klemba, M., Berry, C., Kay, J., and Mottram, J. C. (2001) Aspartic proteases of *Plasmodium falciparum* and other parasitic protozoa as drug targets. Trends Parasitol. 17, 532 – 537.

73 Banerjee, R., Liu, J., Beatty, W., Pelosof, L., Klemba, M., and Goldberg, D. E. (2002) Four plasmepsins are active in the *Plasmodium falciparum* food vacuole, including a protease with an active-site histidine. Proc. Natl. Acad. Sci. USA. 99, 990 – 995.

74 Dunn, B. M. (2002) Structure and mechanism of the pepsin-like family of aspartic peptidases. Chem. Rev. 102, 4431 – 4458.

75 Brik, A., and Wong, C. H. (2003) HIV-1 protease: mechanism and drug discovery. Org. Biomol. Chem. 1, 5 – 14.

76 Berry, C., Humphreys, M. J., Matharu, P., Granger, R., Horrocks, P., Moon, R. P., Certa, U., Ridley, R. G., Bur, D., and Kay, J. (1999) A distinct member of the aspartic proteinase gene family from the human malaria parasite *Plasmodium falciparum*. FEBS Lett. 447, 149 – 154.

77 Villa, J., and Warshel, A. (2001) Energetics and dynamics of enzymatic reactions. J. Phys. Chem. B 105, 7887 – 7907.

78 Åqvist, J., and Warshel, A. (1993) Simulation of enzyme-reactions using valence-bond force-fields and other hybrid quantum-classical approaches. Chem. Rev. 93, 2523 – 2544.

79 Friesner, R. A., and Guallar, V. (2005) Ab initio quantum chemical and mixed quantum mechanics/molecular mechanics (QM/MM) methods for studying enzymatic catalysis. Annu. Rev. Phys. Chem. 56, 389 – 427.

80 Schwede, T., Kopp, J., Guex, N., and Peitsch, M. C. (2003) SWISS-MODEL: an automated protein homology-modeling server. Nucleic Acids Res. 31, 3381 – 3385.

81 Boss, C., Richard-Bildstein, S., Weller, T., Fischli, W., Meyer, S., and Binkert, C. (2003) Inhibitors of the *Plasmodium falciparum* parasite aspartic protease plasmepsin II as potential antimalarial agents. Curr. Med. Chem. 10, 883 – 907.

82 Prade, L., Jones, A. F., Boss, C., Bildstein, S. R., Meyer, S., Binkert, C., and Bur, D. (2005) X-ray structure of plasmepsin II complexed with a potent achiral inhibitor. J. Biol. Chem. 280, 23837 – 23843.

83 Hof, F., Schutz, A., Fah, C., Meyer, S., Bur, D., Liu, J., Goldberg, D. E., and Diederich, F. (2006) Starving the malaria parasite: inhibitors active against the aspartic proteases plasmepsins I, II, and IV. Angew. Chem. Int. Ed. 45, 2138 – 2141.

84 Hulten, J., Bonham, N. M., Nillroth, U., Hansson, T., Zuccarello, G., Bouzide, A., Åqvist, J., Classon, B., Danielson, U. H., Karlen, A., Kvarnstrom, I., Samuelsson, B., and Hallberg, A. (1997) Cyclic HIV-1 protease inhibitors derived from mannitol: synthesis, inhibitory potencies, and computational predictions of binding affinities. J. Med. Chem. 40, 885 – 97.

85 Asojo, O. A., Afonina, E., Gulnik, S. V., Yu, B., Erickson, J. W., Randad, R., Medjahed, D., and Silva, A. M. (2002) Structures of Ser205 mutant plasmepsin II from *Plasmodium falciparum* at 1.8 angstrom in complex with the inhibitors rs367 and rs370. Acta Crystallogr. D Biol. Crystallogr. D 58, 2001 – 2008.

86 Asojo, O. A., Gulnik, S. V., Afonina, E., Yu, B., Ellman, J. A., Haque, T. S., and Silva, A. M. (2003) Novel uncomplexed and complexed structures of plasmepsin II, an aspartic protease from *Plasmodium falciparum*. J. Mol. Biol. 327, 173 – 181.

87 Bernstein, N. K., Cherney, M. M., Loetscher, H., Ridley, R. G., and James, M. N. G. (1999) Crystal structure of the novel aspartic proteinase zymogen proplasmepsin II from *Plasmodium falciparum*. Nat. Struct. Biol. 6, 32 – 37.

88 Silva, A. M., Lee, A. Y., Gulnik, S. V., Majer, P., Collins, J., Bhat, T. N., Collins, P. J., Cachau, R. E., Luker, K. E., Gluzman, I. Y., Francis, S. E., Oksman, A., Goldberg, D. E., and Erickson, J. W. (1996) Structure and inhibition of plasmepsin II, a hemoglobin-degrading enzyme from *Plasmodium falciparum*. Proc. Natl. Acad. Sci. USA. 93, 10034 – 10039.

89 Tyndall, J. D. A., Reid, R. C., Tyssen, D. P., Jardine, D. K., Todd, B., Passmore, M., March, D. R., Pattenden, L. K., Bergman, D. A., Alewood, D., Hu, S. H., Alewood, P. F., Birch, C. J., Martin, J. L., and Fairlie, D. P. (2000) Synthesis, stability, antiviral activity, and protease-bound structures of substrate-mimicking constrained macrocyclic inhibitors of HIV-1 protease. J. Med. Chem. 43, 3495 – 3504.

90 Loughlin, W. A., Tyndall, J. D. A., Glenn, M. P., and Fairlie, D. P. (2004) Beta-strand mimetics. Chem. Rev. 104, 6085 – 6117.

91 Nezami, A., Kimura, T., Hidaka, K., Kiso, A., Liu, J., Kiso, Y., Goldberg, D. E., and Freire, E. (2003) High-affinity inhibition of a family of *Plasmodium falciparum* proteases by a designed adaptive inhibitor. Biochemistry 42, 8459 – 8464.

92 Westling, J., Yowell, C. A., Majer, P., Erickson, J. W., Dame, J. B., and Dunn, B. M. (1997) *Plasmodium falciparum, P. vivax*, and *P. malariae*: a comparison of the active site properties of plasmepsins cloned and expressed from three different species of the malaria parasite. Exp. Parasitol. 87, 185 – 193.

93 Bernstein, N. K., Cherney, M. M., Yowell, C. A., Dame, J. B., and James, M. N. (2003) Structural insights into the activation of *P. vivax* plasmepsin. J. Mol. Biol. 329, 505 – 524.

94 Clemente, J. C., Govindasamy, L., Madabushi, A., Fisher, S. Z., Moose, R. E., Yowell, C. A., Hidaka, K., Kimura, T., Hayashi, Y., Kiso, Y., Agbandje-McKenna, M., Dame, J. B., Dunn, B. M., and McKenna, R. (2006) Structure of the aspartic protease plasmepsin 4 from the malarial parasite *Plasmodium malariae* bound to an allophenylnorstatine-based inhibitor. Acta Crystallogr. D. Biol. Crystallogr. 62, 246 – 252.

95 Marelius, J., Hansson, T., and Åqvist, J. (1998) Calculation of ligand binding free energies from molecular dynamics simulations. Int. J. Quantum Chem. 69, 77 – 88.

96 Åqvist, J., and Hansson, T. (1996) On the validity of electrostatic linear response in polar solvents. J. Phys. Chem. 100, 9512 – 9521.

97 Miller, M., Schneider, J., Sathyanarayana, B. K., Toth, M. V., Marshall, G. R., Clawson, L., Selk, L., Kent, S. B. H., and Wlodawer, A. (1989) Structure of complex of synthetic HIV-1 protease with a substrate-based inhibitor at 2.3 Å resolution. Science 246, 1149 – 1152.

98 Kiso, A., Hidaka, K., Kimura, T., Hayashi, Y., Nezami, A., Freire, E., and Kiso, Y. (2004) Search for substrate-based inhibitors fitting the S-2' space of malarial aspartic protease plasmepsin II. J. Pept. Sci. 10, 641 – 647.